

Article

The Effects of Lactose Induction on a Plasmid-Free *E. coli* T7 Expression System

Johanna Hausjell ^{1,†}, Regina Kutscha ^{1,†}, Jeannine D. Gesson ², Daniela Reinisch ² and Oliver Spadiut ^{1,*} 

¹ TU Wien, Institute of Chemical, Environmental and Bioscience Engineering, Research Division Biochemical Engineering, 1060 Vienna, Austria; johanna.hausjell@tuwien.ac.at (J.H.); regina_phf1@yahoo.de (R.K.)

² Boehringer Ingelheim RCV GmbH & Co KG, 1120 Vienna, Austria; jeannine.gesson@boehringer-ingelheim.com (J.D.G.); daniela.reinisch@boehringer-ingelheim.com (D.R.)

* Correspondence: oliver.spadiut@tuwien.ac.at; Tel.: +43-1-58801-166473; Fax: +43-1-58801-166980

† These authors contributed equally to this work.

Received: 5 November 2019; Accepted: 3 January 2020; Published: 6 January 2020



Abstract: Recombinant production of pharmaceutical proteins like antigen binding fragments (Fabs) in the commonly-used production host *Escherichia coli* presents several challenges. The predominantly-used plasmid-based expression systems exhibit the drawback of either excessive plasmid amplification or plasmid loss over prolonged cultivations. To improve production, efforts are made to establish plasmid-free expression, ensuring more stable process conditions. Another strategy to stabilize production processes is lactose induction, leading to increased soluble product formation and cell fitness, as shown in several studies performed with plasmid-based expression systems. Within this study we wanted to investigate lactose induction for a strain with a genome-integrated gene of interest for the first time. We found unusually high specific lactose uptake rates, which we could attribute to the low levels of lac-repressor protein that is usually encoded not only on the genome but additionally on pET plasmids. We further show that these unusually high lactose uptake rates are toxic to the cells, leading to increased cell leakiness and lysis. Finally, we demonstrate that in contrast to plasmid-based T7 expression systems, IPTG induction is beneficial for genome-integrated T7 expression systems concerning cell fitness and productivity.

Keywords: *E. coli*; T7 expression system; plasmid-free expression; lactose induction; antigen binding fragment (Fab); lac-repressor (LacI)

1. Introduction

E. coli is one of the most widely used hosts for recombinant protein production to date. Genetic manipulation is easy and versatile, there are numerous strains and plasmids available, and the cells can be cultivated fast, in cheap media, to high cell densities [1–5].

Conventionally, plasmids are used for recombinant protein production in *E. coli*, including the most frequently employed pET vectors, commercially established by NovagenTM. On pET plasmids, the gene of interest (GOI) is encoded under control of the T7 promoter, which is recognized by T7 RNA polymerase. Compatible strains like *E. coli* BL21 (DE3), have the λ DE3 region integrated into the genome, where transcription of T7 RNA polymerase is controlled by the *lacUV5* promoter. Therefore, transcription and translation of the GOI depends upon transcription and translation of the T7 RNA polymerase from the *lacUV5* promoter. Before induction, transcription of the T7 RNA polymerase and consequently the GOI are inhibited by the lac-repressor (LacI) which binds in a tetrameric structure to the respective operator sites [6]. *Lac* operator sites are located in (I) the native *E. coli lac* promoter (II) the *lacUV5* promoter, which regulates transcription of the T7 RNA polymerase and (III) in the *lac* operator

regions included downstream of the T7 promoter and upstream of the translation initiation sequence of the GOI for ensuring tighter transcription control [6]. A copy of *lacI* is present in the genomic DNA of the cell as well as on pET plasmids. During induction, the LacI-tetramer is bound by allolactose or one of its analogs, dissociates from the operator-sites and enables transcription and translation of the T7 RNA polymerase and thus in turn expression of the GOI from the T7 promoter [7–9].

Unfortunately, plasmid-based expression systems exhibit certain drawbacks. They either (I) tend to amplify the plasmid copy number in prolonged cultivations, or (II) plasmids are lost over time, propagating the segregation of a plasmid-free sub-population during induction. The latter has also been described in context with T7-pET systems, making establishment of stable production processes challenging [10,11].

One way to overcome these challenges is employment of plasmid-free expression systems, where the GOI is integrated directly into the host genome. A number of recombination methods have been developed for establishment of such systems and different suitable chromosomal integration sites in *E. coli* have been investigated [12,13]. Once the GOI is integrated into the genome, recombinant production is no longer subject to plasmid number variations, allowing, aside from stable processes, the establishment of a reference for the performance of plasmid-based systems as well. However, one of the major drawbacks of moving away from plasmid-based systems remains, leading to a slightly limited production capacity due to the lowered copy number of the GOI [1,14–16].

The gold standard for induction in T7 expression systems is IPTG, as it ensures stable and strong induction since it is not metabolized by the cells. This makes one point addition sufficient, easing handling of bioprocesses. Nevertheless, it has been reported that IPTG puts a high metabolic burden on the cells, decreases the amount of soluble recombinant protein, and exacerbates substrate toxicity [17–19]. One way to tackle these adverse effects is to use lactose as inducer, which has been shown to yield in similar if not higher product titers and to increase soluble product formation and cell fitness, enabling longer production times [19–22]. Additionally, lactose is cheap and non-toxic. Nevertheless, it has to be kept in mind that the disaccharide has to be supplied constantly, as it is rapidly metabolized by the cells.

Recent studies from our group showed that there is a correlation between the maximum specific lactose uptake rate ($q_{s,lac,max}$) and the specific glucose uptake rate ($q_{s,glu}$) in *E. coli* BL21 (DE3) strains carrying pET plasmids. For several different pET plasmids for expression of various products, a mechanistic model for this correlation has been established, which can serve as a basis for steering product titers, product properties and/or product location [20,23,24].

Within this study we wanted to investigate the potential differences in the correlation between $q_{s,glu}$ and $q_{s,lac,max}$ for a strain where the GOI was not located on a pET plasmid but genome-integrated, knowledge which has not been generated to date. We wanted to shed light on the role of the plasmid and investigate if differences in the correlation were detectable when switching from plasmid-based to genome-integrated systems. As a model protein FabZ, an antigen binding fragment (Fab), was used which was translocated into the periplasm, as the oxidizing environment there allows necessary formation of disulfide bonds. As it is well known that periplasmic protein production can lead to cell leakiness and lysis [25], we further investigated if lactose induction had a positive effect in this regard. Finally, we compared induction by lactose to a standard IPTG-induced FabZ production process concerning productivity as well as physiology and viability.

2. Materials and Methods

2.1. Strains

In this study we used an *E. coli* BL21 (DE3) strain, which was provided by Boehringer Ingelheim RCV. The genes for the FabZ heavy chain and the FabZ light chain were encoded under the control of the T7 promoter and integrated into the genome at the attTN7 site by recombineering according to [26]. The homologous overhangs were each approximately 50 bp. Each gene was preceded by an

ompA leader sequence (signal sequence for translocation into the periplasm) and a ribosomal binding site for efficient translation. A bicistronic mRNA was used, where the T7 promoter is followed by the open reading frame of the light chain including the *ompA* leader sequence and subsequently the open reading frame of the heavy chain also including the *ompA* leader sequence. Additionally, the strain carried a kanamycin-resistance. The ribosome binding site used was aagaaggaga. The *ompA*-leader sequence was MKKTAIAIAVALAGFATVAQA in terms of amino acids, the respective DNA-sequence was optimized together with the light and heavy chain of FabZ. Sequence details of the product FabZ are confidential. The heavy chain is 23.2 kDa and has a pI between 9.05 and 9.06 (depending on the prediction tools used), the light chain is 23.1 kDa and has a pI between 5.62 and 5.74. The full construct is 46.3 kDa and has a pI of 8.41. The overall integration cassette consisted of the T7-promoter, the ribosome binding site, *ompA*-light chain, ribosome binding site, *ompA*-heavy chain, the T7-terminator and a kanamycin resistance gene. Regarding the promoter, terminator, *ompA* and the kanamycin resistance gene, standard sequences were used.

To study the influence of the lac-repressor (LacI), the strain was transformed with an empty pET-21 d (+) plasmid in the course of our investigation.

2.2. Transformation with pET-21 d (+)

A heat-shock transformation of *E. coli* BL21(DE3) with pET-21 d (+) was performed. In order to produce chemically competent cells, the cells were grown in LB-medium at 37 °C and 230 rpm to an optical density of about 0.5 at 600 nm. After centrifugation (2500× *g*, 4 °C, 10 min) the supernatant was discarded and the cells were resuspended in 2 mL of ice-cold 30 mM CaCl₂. Subsequently, the cells were spun down for 30 s and the pellet was gently resuspended in 0.5 mL of ice-cold 30 mM CaCl₂.

50 µL of this cell-suspension were mixed with 3 µL (442 ng) of plasmid DNA and incubated on ice for 30 min. Then the mixture was incubated at 42 °C for 30 s and then on ice for 5 min. Next, 950 µL of SOC-medium (0.5% yeast extract, 2% tryptone, 10 mM NaCl, 2.5 mM KCl, 10 mM MgCl₂, 10 mM MgSO₄, and 20 mM glucose) were added, and the cells were regenerated at 30 °C and 180 rpm for 1 h.

For selection, the cells were grown on LB-agar plates containing 50 µg/mL kanamycin and 100 µg/mL ampicillin at 30 °C for 72 h. Successful transformation of the cells with the plasmid was confirmed by isolation and commercial sequencing (Microsynth Austria AG, Vienna, Austria).

2.3. Bioreactor Cultivations

Cultivations were carried out once in the controlled environment of a bioreactor, closing C-balances were used as a control for calculations. Measurements and analyses of samples were carried out in triplicates. All bioreactor cultivations included a batch phase, an uninduced fed-batch phase to a dry cell weight concentration of 30 g/L, and an induction phase of 6 h.

Cultivations were performed in DASbox[®] Mini Bioreactors (Eppendorf, Hamburg, Germany) with 250 mL working volume. The pH was measured via pH-Sensor EasyFerm Plus (Hamilton, Reno, NV, USA) probes, dissolved oxygen with Visiferm DO 120 electrodes (Hamilton, Reno, NV, USA), and CO₂ and O₂ in the offgas via a DASGIP[®] GA gas analyzer (Eppendorf, Hamburg, Germany). For aeration a mixture of pressurized air and pure oxygen was provided at 18 L/h. The stirring speed was kept at 2000 rpm. The dissolved oxygen saturation was held above 30% by adding more pure oxygen if required. The feed-flowrates were regulated via a DASbox[®] MP8 Multi Pump Module, the pH was kept at 6.8 during batch and fed-batch phase, and was adjusted to 7.1 during the induction phase. The temperature was controlled at 37 °C during the growth phases and subsequently lowered to 32 °C for the induction phase. The process parameters were recorded and controlled by DASware[®] control.

Five hundred milliliters of DeLisa pre-culture medium [27], containing 30 mg/L kanamycin, were inoculated aseptically with one frozen stock of cells (−80 °C; 1.5 mL) and incubated overnight (approximately ~17 h) in 2500 mL high-yield shake flasks at 37 °C and 200 rpm. The DeLisa batch medium was inoculated with 10% of the starting volume. After the sugar was depleted, indicated by a drop in the CO₂ signal, the biomass concentration was further increased (to approximately 30 g/L)

by carrying out a fed-batch phase with a glucose feed of 400 g/L. The production of FabZ was either induced with 1.25 mM IPTG, as used the industrially developed process, following an induction phase with an average $q_{s,glu}$ of 0.13 g/g/h, or, for lactose induction, two feeds including a 400 g/L glucose feed as well as a 200 g/L lactose feed were utilized to achieve the desired specific sugar uptake rates.

2.4. Feed Control Strategy

The amount of feed added to the reactors for exponential fed-batch phases was calculated by the control software using a simple feed-forward exponential feeding strategy, according to the following equation:

$$\text{Feed setpoint} \left[\frac{mL}{h} \right] = q_s * V * c_x * e^{(\mu * t)} * \frac{1000}{c_s}. \quad (1)$$

μ specific growth rate on glucose/lactose [h^{-1}]

q_s specific glucose/lactose uptake rate [$g_x/g_s/h$]

V reactor volume [L]

c_x biomass concentration [g_x/L]

t time [h]

c_s concentration of the feed [g_s/L]

The growth rate was calculated from the specific sugar uptake rates and yields on the respective sugars.

2.5. Sampling

Samples were taken at the start of the batch phase, at the start of the fed-batch phase, at the beginning of the induction, and in different intervals during induction. For cultivations needed for the correlation between $q_{s,glu}$ and $q_{s,lac,max}$ the sampling interval was one hour, for further experiments concerning tunability and the influence of LaCl the sampling interval was widened to 6 h. For every sample the optical densities at 600 nm (OD_{600}) and at 550 nm (OD_{550}) were determined spectroscopically using a Genesys 20 photometer (Thermo Scientific, Waltham, MA, USA), using appropriate dilutions to stay in the linear range (OD_{600} 0.2–0.8).

Biomass aliquots of each sample were generated by pipetting an amount of cell broth calculated via Equation (2),

$$\text{sample volume [mL]} = \frac{10}{OD_{550}}, \quad (2)$$

into 500 μ L of 0.9% NaCl solution.

These aliquots were then centrifuged at 20,000 \times g at 4 $^{\circ}$ C for 10 min in a Sigma 3-18K centrifuge. The supernatant was discarded and the samples were frozen at -20 $^{\circ}$ C for product analytics.

Dry cell weight was determined gravimetrically by pipetting 1 mL of sample into pre-weighed 2 mL Eppendorf tubes, centrifuging at 20,000 \times g at 4 $^{\circ}$ C for 10 min using a Sigma 3-18K centrifuge (Sigma Laborzentrifugen GmbH, Osterode am Harz, Germany), resuspending the pellet in 1 mL of 0.9% NaCl, centrifuging again at the same conditions and drying the pellets at 110 $^{\circ}$ C for 72 h. Subsequently, the pellets were weighed.

Additionally, at the end of the cultivation, several 10 mL samples of culture broth were taken, centrifuged at 5000 \times g for 30 min at 4 $^{\circ}$ C and the pellet was frozen at -20 $^{\circ}$ C for later homogenization.

The concentrations of glucose, lactose, galactose, and acetate were determined via HPLC in the cell-free supernatant (Thermo Fisher Scientific, Waltham, MA USA) with an Aminex HPX-87H Column (Bio-Rad, Hercules, CA, USA) using 4 mM H_2SO_4 for isocratic separation and a RefractoMax520 refractive index detector (DataApex, Petržilkova, Prague, Czech Republic). The flowrate was set to 0.6 mL/min and the method lasted for 30 min. All analyses were performed in triplicates.

2.6. Product Analytics

Product analytics of soluble product in the cells and in the cell-free supernatant were carried out according to procedures previously described in literature [28].

2.7. Leakiness (Alkaline Phosphatase Assay)

Within our study the term “leakiness” refers to cells where alkaline phosphatase and FabZ can be detected in the culture supernatant, indicating a permeable outer membrane. This includes cells, which are lysed and have an open outer membrane for this reason. However, we additionally determined DNA contents in the culture supernatant, which rise upon cell lysis. To determine cell leakiness, an alkaline phosphatase assay was performed with the cell-free supernatants according to literature [25]. For comparability reasons between different cultivations, the slopes of the measurements were divided by the biomass concentration.

Additionally, cells were homogenized by resuspending the pellets from the 10 mL samples in buffer A (20 mM $\text{NaH}_2\text{PO}_4 \cdot 2\text{H}_2\text{O}$, 100 mM NaCl, pH 7) and running 10 passages at approximately 1000 bar in a Panda Plus Homogenizer (GEA Niro Soavi, Parma, Italy). After the subsequent centrifugation at $15,000 \times g$ and 4°C for 20 min, alkaline phosphatase activity was measured in the supernatant. The slopes of these measurements were again normalized by biomass used for homogenization. The resulting values were defined as 100% leakiness for the different cultivations.

2.8. Lysis (Picogreen Assay)

To estimate the amount of lysed cells, Quant-iT™ PicoGreen® dsDNA assays (Invitrogen™, Thermo Fisher Scientific, Waltham, MA USA) were performed using a Quant-iT™ PicoGreen™ dsDNA Assay Kit. After preparing a working solution (200-fold dilution of the concentrated DMSO solution of Quant-iT™ PicoGreen® reagent in TE-buffer (10 mM Tris-HCl, 1 mM EDTA, pH 7.5)), 100 μL thereof were mixed with 100 μL of 100-fold diluted cell-free supernatant and incubated in the dark at room temperature for 5 min. Fluorescence was measured by exciting at 480 nm and measuring the emission at 520 nm using an Infinite 200 Pro plate reader (Tecan, Zürich, Switzerland). The calibration was done with the lambda DNA standard provided in the assay kit in a range of 1 ng/mL to 1 $\mu\text{g/mL}$. In order to compare the results of different cultivations at different times, the resulting DNA-concentrations were normalized by biomass.

3. Results and Discussion

3.1. Correlation between $q_{s,glu}$ and $q_{s,lac,max}$

We wanted to shed light on the mechanistic correlation between the specific glucose uptake rate ($q_{s,glu}$) and the maximum specific lactose uptake rate ($q_{s,lac,max}$) for a genome-integrated FabZ *E. coli* BL21 (DE3) strain (hereafter referred to as GI-strain). Previously, this correlation had only been recorded for plasmid-based T7 expression systems, where results showed that the correlation differed, dependent on the pET-plasmid and the expressed protein (Figure 1a) [23].

To determine the correlation between $q_{s,glu}$ and $q_{s,lac,max}$ for the GI strain, bioreactor cultivations at different $q_{s,glu}$ set-points were carried out while supplying lactose in excess. The excess lactose supply was confirmed by HPLC-measurements, where lactose was detected in the supernatant of the culture broth at quantities greater than 0.5 g/L at all times. The actual specific lactose uptake rate was determined after an adaption phase ranging from 2 h to 5 h, which depended on the specific glucose uptake rate. The end of the adaption phase was indicated by a subsequently constant $q_{s,lac,max}$.

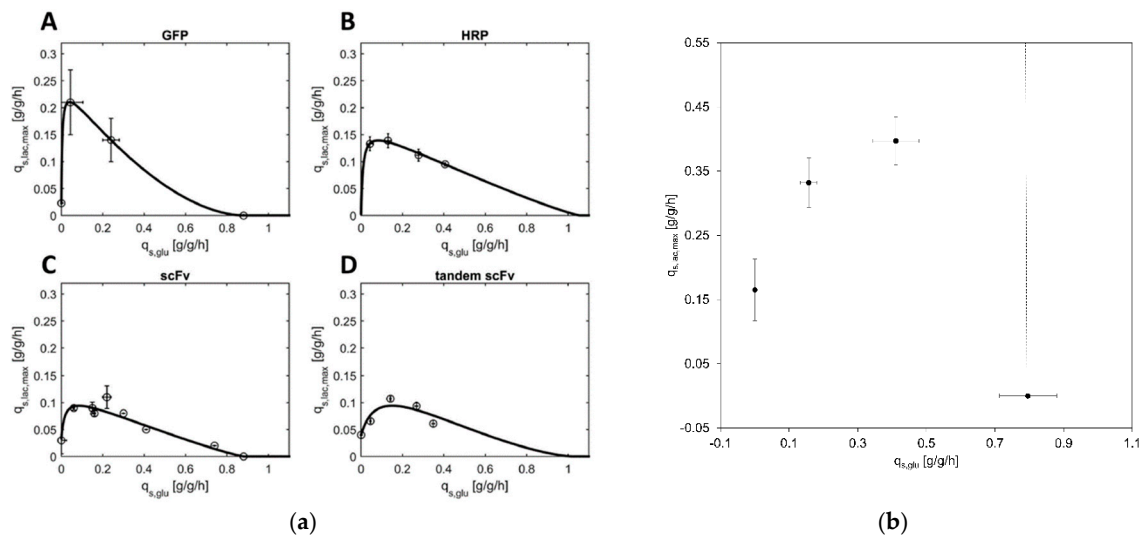


Figure 1. $q_{s,glu}/q_{s,lac,max}$ -correlations (a) $q_{s,glu}/q_{s,lac,max}$ -correlation for recombinant pET-based *E. coli* BL21 (DE3) strains producing either (A) GFP, (B) HRP, (C) the scFv or (D) the tandem scFv. Data-points were obtained from batch and fed-batch cultivations with constant $q_{s,glu}$ and excess lactose (“static experiments”) and subsequently fitted to the mechanistic model (Equation (1)) reprinted from [23] as a comparison to previously recorded correlations between $q_{s,glu}$ and $q_{s,lac,max}$ for plasmid-containing BL21 (DE3) strains. (b) $q_{s,lac,max}$ as a function of $q_{s,glu}$ for the GI strain; the data-points were gained from the different batch and fed-batch cultivations: Point 1 ($q_{s,lac,max}$ 0.17 ± 0.05 g/g/h at $q_{s,glu}$ 0 g/g/h) is derived from a fed-batch only on lactose, the two middle points ($q_{s,lac,max}$ 0.33 ± 0.05 g/g/h at $q_{s,glu}$ 0.19 ± 0.04 g/g/h; $q_{s,lac,max}$ 0.40 ± 0.04 g/g/h at $q_{s,glu}$ 0.41 ± 0.07 g/g/h) were calculated from fed-batch cultivations where limiting amounts of glucose were fed and lactose was provided in excess, and point 4 (on the right) indicates the value of the maximum specific glucose uptake rate. Above this point, also indicated by a dotted line, glucose would accumulate and therefore no lactose uptake would occur due to the well-known phenomenon of diauxic growth and carbon catabolite repression whenever glucose and lactose are present in excess e.g., [29–31]. The error bars indicate the standard deviation of $q_{s,glu}$ and $q_{s,lac,max}$ during the cultivations.

Based on previously recorded $q_{s,glu}$ - $q_{s,lac,max}$ correlations for plasmid-carrying *E. coli* BL21 (DE3) [23], we expected very little lactose uptake ($q_{s,lac,max}$ below 0.05 g/g/h) in the complete absence of glucose. Additionally, we expected the highest $q_{s,lac,max}$ at a specific glucose uptake rate of about 0.1 to 0.2 g/g/h. At those values usually $q_{s,lac,max}$ of 0.1 to 0.2 g/g/h were reached (Figure 1a).

However, as shown in Figure 1b, the correlation for the GI strain differed strongly. In contrast to plasmid-based systems, where we detected almost no capability for lactose uptake if glucose was absent ($q_{s,lac,max} < 0.05$ g/g/h), we noticed considerable cell growth (Supplementary Table S1) and lactose uptake in the GI strain without supplementation of glucose ($q_{s,lac,max} = 0.17$ g/g/h).

Aside from this astonishingly high lactose uptake in the absence of glucose, we also observed differences in the maximum of the $q_{s,glu}$ - $q_{s,lac,max}$ correlation. With 0.40 g/g/h, the highest $q_{s,lac,max}$ of the GI strain was almost double the amount of the highest previously recorded $q_{s,lac,max}$, which was just above 0.2 g/g/h for an *E. coli* BL21 (DE3) strain, expressing green fluorescent protein from a pET-21 a (+) plasmid. Further, the highest $q_{s,lac,max}$ of the GI strain occurred at clearly elevated $q_{s,glu}$ -values. While in plasmid-based systems the highest $q_{s,lac,max}$ correlates to $q_{s,glu}$ values between 0.1 and 0.2 g/g/h, the highest $q_{s,lac,max}$ recorded for the GI strain is found at a $q_{s,glu}$ of 0.41 g/g/h. Unfortunately, we were not able to determine $q_{s,lac,max}$ -values at higher $q_{s,glu}$, since the cells tended to get leaky and lyse very quickly (in a matter of about 6 h; Figure 2a) if exposed to excess lactose for a prolonged time. Consequently, the cells had barely any time to fully adapt to lactose before lysing and there was no possibility to analyze the correlation at higher $q_{s,glu}$ points, rendering a mechanistic modelling, as it has been done before [23], impossible.

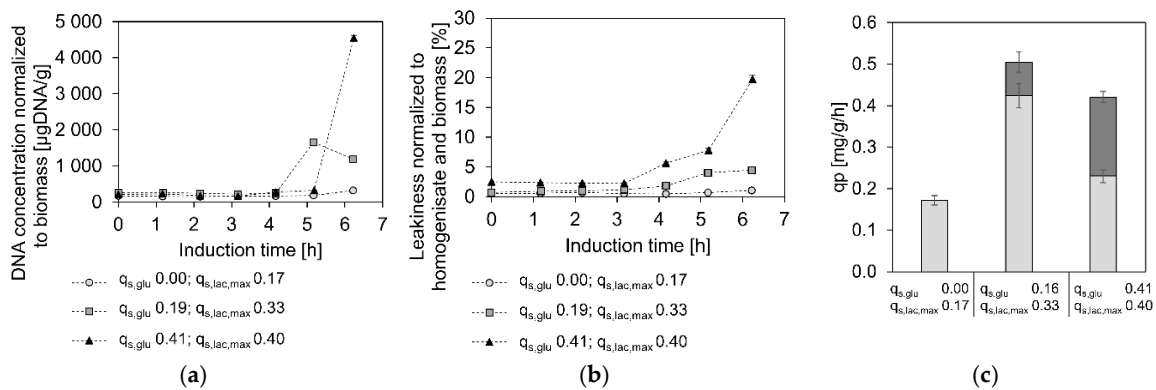


Figure 2. Leakiness, lysis and productivity at different $q_{s,glu}/q_{s,lac,max}$ (a) Lysis normalized to biomass at the different $q_{s,glu}$ and correlating $q_{s,lac,max}$ values: black triangles indicate values for $q_{s,glu} = 0.41$ g/g/h $q_{s,lac,max} = 0.40$ g/g/h, grey squares represent $q_{s,glu} = 0.19$ g/g/h $q_{s,lac,max} = 0.33$ g/g/h, light grey circles are values obtained from the lactose batch experiment. (b) Leakiness normalized to biomass: Black triangles indicate values for $q_{s,glu} = 0.41$ g/g/h $q_{s,lac,max} = 0.40$ g/g/h, grey squares represent $q_{s,glu} = 0.19$ g/g/h $q_{s,lac,max} = 0.33$ g/g/h, light grey circles are values obtained from the lactose batch experiment. (c) specific overall, intracellular (light grey), and extracellular (dark grey) product formation rates for the $q_{s,glu}$ and correlating $q_{s,lac,max}$ values.

Nevertheless, we investigated productivity at the different points along the $q_{s,lac,max}$ – $q_{s,glu}$ correlation curve. As shown in Figure 2c, the highest overall specific soluble product formation rate (q_p) was detected at a medium $q_{s,glu}$ of 0.19 g/g/h and a $q_{s,lac,max}$ of 0.33 g/g/h. The cultivation at a $q_{s,glu}$ of 0.41 g/g/h and a $q_{s,lac,max}$ of 0.40 g/g/h yielded less FabZ per biomass and hour and the lactose batch cultivation only exhibited a q_p below 0.2 mg/g/h. The overall trend, that q_p is lower when little glucose is taken up but also when $q_{s,glu}$ is high, is the same, as previously found for plasmid-based systems [24], although it has to be kept in mind, that only soluble product was investigated in this study.

Interestingly, the q_p loss due to extracellular product clearly increased with higher specific lactose and glucose uptake rates. This most likely results from cell leakiness and lysis, as both seem to increase similarly at higher sugar uptake rates (Figure 2a,b). We hypothesized that at high specific lactose uptake rates the so-called lactose killing was triggered [32]. This phenomenon describes the death of *E. coli* grown on excess lactose and has been attributed to the transport of lactose through the cell membrane, influencing the proton motif force and leading to cell death [33]. In our case, the high specific glucose uptake rates and product formation in the periplasm might have additionally promoted cell lysis.

Summing up, we found similar trends for the productivity of the GI strain and plasmid-based expression systems along the $q_{s,lac,max}$ – $q_{s,glu}$ correlation curve, however, the curve of the GI strain itself was clearly higher and its maximum was shifted to the right. Previous cultivations for the plasmid based expression systems were carried out at 30 °C, however, we chose 32 °C for the induction of FabZ expression, as this was determined as optimal induction temperature for this protein. Although sugar uptake rates and growth rates rise with higher temperatures, we found it rather unlikely that rising the temperature by 2 °C was the cause for almost doubling the lactose uptake rates.

Instead, we hypothesized that the reason for this strong divergence could originate from the plasmids. All employed pET plasmids from our previous studies [20,23,24,34] were high copy number plasmids, which also carried a *lacI* gene, thereby introducing much more repressor protein into the cells. The GI strain however, only expressed LacI from the copies in the genome [35]. Consequently, in the GI strain, less LacI would bind to the *lac* promoter and expression of lactose permease was elevated, allowing higher specific lactose uptake rates.

3.2. The Influence of *LacI*

To test our hypothesis that the GI strain exhibited higher $q_{s,lac,max}$ values compared to plasmid-based systems, as a result of less *lacI* copies, an empty pET-21 d (+) plasmid was introduced into the GI strain. The high copy number plasmid carried an additional *lacI* gene. The transformed cells were cultivated in a bioreactor under the same conditions as before with an excess of lactose, at a $q_{s,glu}$ comparable to 0.19 g/g/h. Specific sugar uptake rates, productivity, and leakiness/lysis were evaluated for the plasmid containing GI strain and compared to previous results of the GI strain without plasmid (Figure 3).

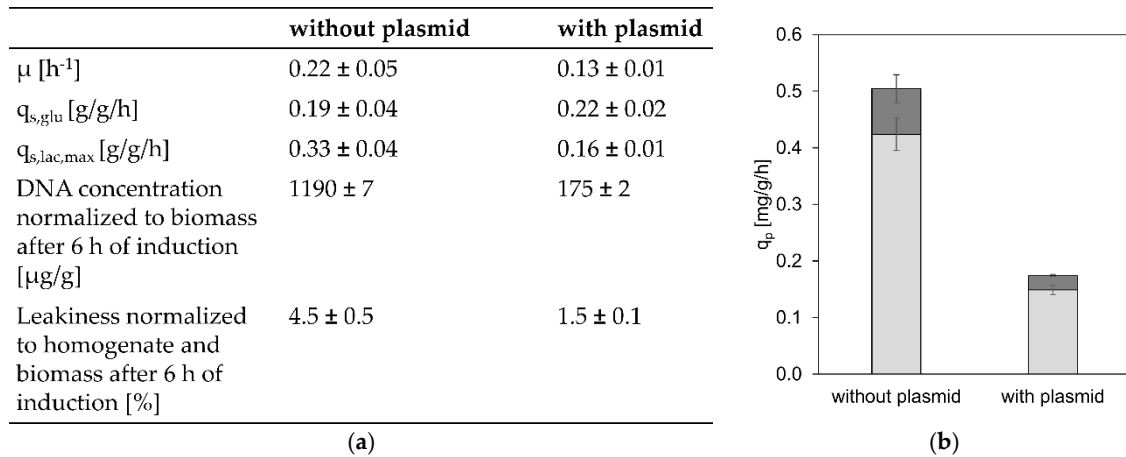


Figure 3. Physiology, leakiness, lysis and productivity for the GI-strain with and without an additional pET plasmid. (a) Comparison of physiological data as well as leakiness and lysis of a cultivation of the GI strain without plasmid and the GI strain containing the empty pET-21 d (+) plasmid; (b) Specific overall, intracellular (light grey), and extracellular (dark grey) product formation rates compared between the cultivations with and without plasmid.

At a comparable $q_{s,glu}$, the plasmid-containing strain exhibited only a $q_{s,lac,max}$ of 0.16 g/g/h, approximately half of that of the GI strain without the plasmid and in the range of previously recorded $q_{s,lac,max}$ values, which were found between 0.1 and 0.2 g/g/h. This confirmed our hypothesis that the shift in the $q_{s,lac,max}$ - $q_{s,glu}$ correlation of the GI strain was a result of the reduced number of *lacI* copies.

In accordance with sugar uptake rates, productivity and cell lysis differed for the plasmid containing GI strain as well. Productivity was clearly reduced as a result of less T7 RNA polymerase expression from the *lacUV5* promoter and cell lysis and leakiness were decreased as well, which we hypothesized could either be an effect of the lower specific lactose uptake rate or the lower amount of product in the periplasm of the cells.

3.3. Toxicity of High Lactose Uptake Rates

As including a pET-21 d (+) plasmid containing a *lacI* copy in the GI strain led to less cell lysis and leakiness, we were interested if the reason for this was the reduced productivity, putting less stress on the cells or the lower specific lactose uptake rate. For closer investigation we decided to perform two cultivations at the same $q_{s,glu}$ (0.14 g/g/h) and at 100% $q_{s,lac,max}$ as well as approximately 60% of $q_{s,lac,max}$, as it has previously been shown that reducing $q_{s,lac,max}$ to 57% still leads to comparable specific product formation rates (95.5% target protein) [20]. Results are shown in Figure 4.

As shown in Figure 4b, indeed a similar overall q_p was reached in both cultivations (88% of the q_p at 100% $q_{s,lac,max}$ was still reached at 60% $q_{s,lac,max}$). However, in the cultivation at 60% $q_{s,lac,max}$ more product is found intracellularly and less in the cultivation supernatant. This is a result of less cell lysis and leakiness as shown in Figure 4a, indicating that not recombinant protein production but the high lactose uptake rates are toxic for the cells.

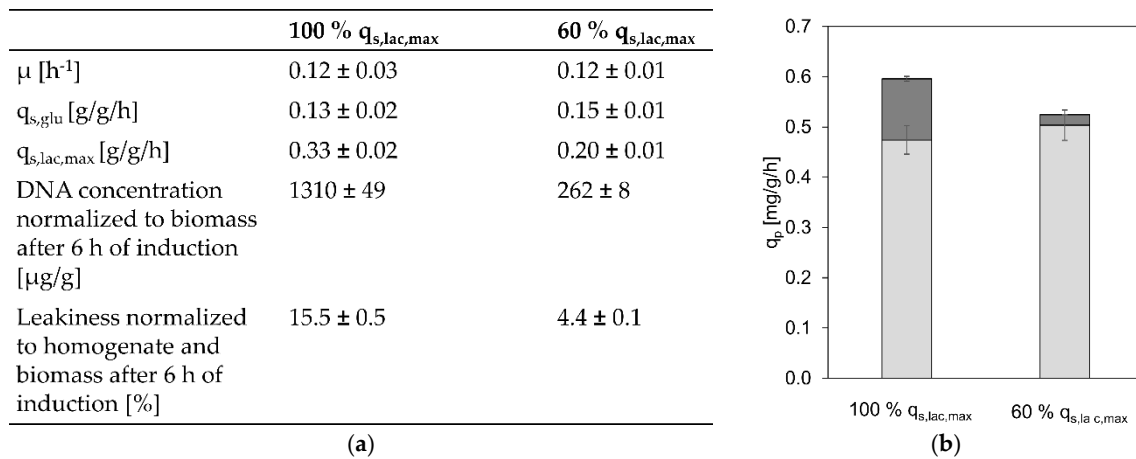


Figure 4. Physiology, leakiness, lysis and productivity at 100% and 60% $q_{s,lac,max}$ (a) Comparison of physiological data as well as leakiness and lysis of a cultivation at a $q_{s,glu}$ 0.14 g/g/h and different $q_{s,lac}$ (100% $q_{s,lac,max}$ and 60% $q_{s,lac,max}$); (b) specific overall, intracellular (light grey), and extracellular (dark grey) product formation rates of cultivations at 100% $q_{s,lac,max}$ and 60% $q_{s,lac,max}$.

3.4. Comparison between Lactose Induction and IPTG Induction

For plasmid-based systems it has been reported that lactose induction provided the advantages of increased soluble product formation and cell fitness [19–22]. However, as the high specific lactose uptake rates of the GI strain clearly seemed toxic to the cells, we wanted to check if perhaps IPTG induction was beneficial for this strain. Therefore, we compared data obtained from the cultivation with lactose induction resulting in the highest q_p to an IPTG-induced cultivation that was conducted at a similar $q_{s,glu}$. For comparability, both inducers were provided in excess. The physiological parameters as well as the specific product formation rates and the cell-lysis data are shown in Figure 5.

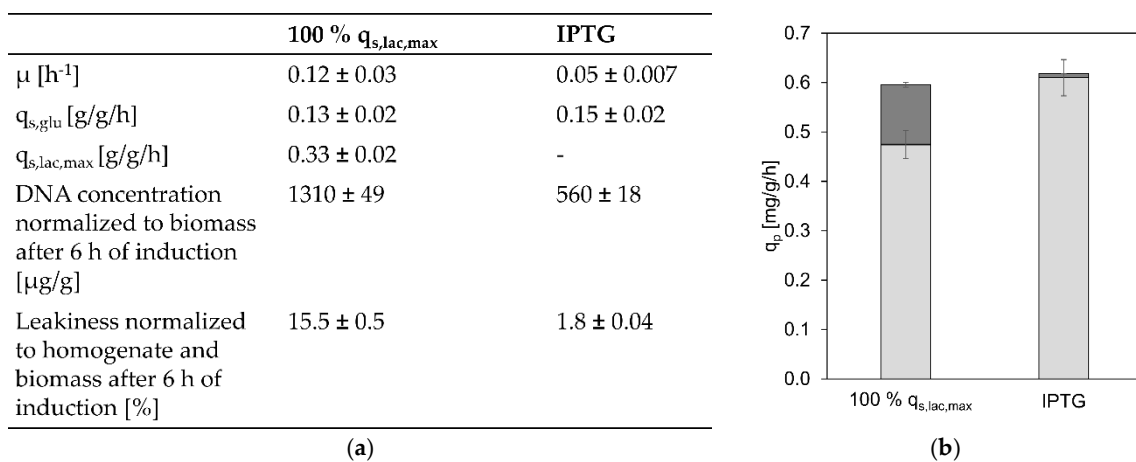


Figure 5. Physiology, leakiness, lysis, and productivity when inducing FabZ production by lactose or IPTG. (a) Comparison of physiological data as well as cell lysis and leakiness of the lactose induction cultivation at which the highest q_p was reached and an IPTG-induced cultivation conducted at the same $q_{s,glu}$; (b) specific overall, intracellular (light grey), and extracellular (dark grey) product formation rates of the lactose-induced cultivation at which the highest q_p was reached and an IPTG-induced cultivation conducted at the same $q_{s,glu}$.

As shown in Figure 5, the overall q_p is similar in the lactose and the IPTG-induced process, however, the extracellular product formation is clearly reduced in the IPTG-induced process in comparison to lactose-induced cells. This most likely is a result of less cell lysis and leakiness in the IPTG-induced cultivation as shown in Figure 5a. All of this indicates that for a GI strain, with the GOI

under control of the T7 promoter, lactose induction does not provide the same advantages which were previously discovered for plasmid-based systems. On the contrary, it seems to slightly reduce overall productivity and clearly diminishes cell viability compared to IPTG induction.

4. Conclusions

In this study we investigated the effects of lactose induction on an *E. coli* BL21 (DE3) expression system with a genome-integrated GOI. Previously, only plasmid-based expression systems had been subject to studies investigating lactose as an inducer for recombinant protein production [23,36,37]. In those studies, beneficial effects on productivity, cell fitness, viability, and soluble product formation had been reported [21,22,38–40].

Within this study we showed, for the first time, that an *E. coli* BL21 (DE3) expression system with a genome-integrated GOI showed specific maximum lactose uptake rates that were more than double as high compared to pET-plasmid based systems. We demonstrated that this difference is caused by the lack of a plasmid carrying additional copies of *lacI* and further showed that these unusually high lactose uptake rates of more than 0.4 g/g/h were toxic to the cells leading to increased cell lysis and product loss in the supernatant. Therefore, we conclude that previously discovered benefits of lactose induction are not applicable to strains with genome integrated GOIs under control of the T7 promoter.

Supplementary Materials: The following are available online at <http://www.mdpi.com/2306-5354/7/1/8/s1>, Table S1: Physiological parameters of cultivations at $q_{s,lac,max}$ at different $q_{s,glu}$.

Author Contributions: Conceptualization, O.S.; methodology, O.S. and J.H.; software, J.H.; validation, J.H. and R.K.; formal analysis, R.K.; investigation, J.H. and R.K.; resources, J.D.G. and D.R.; writing—original draft preparation, R.K. and J.H.; writing—review and editing, J.H., O.S., J.D.G. and D.R.; visualization, J.H. and R.K.; supervision, O.S. and D.R.; project administration, O.S., J.D.G. and D.R.; funding acquisition, O.S. All authors have read and agreed to the published version of the manuscript.

Funding: This research was funded by Boehringer Ingelheim RCV GmbH and Co KG.

Acknowledgments: The authors are very grateful to Martin Voigtmann and team for evaluation of Fab-expression levels. The authors acknowledge TU Wien Bibliothek for financial support through its Open Access Funding by TU Wien.

Conflicts of Interest: J.D.G. and D.R. were employees of Boehringer Ingelheim RCV GmbH & Co KG when this study was conducted.

References

1. Jia, B.; Jeon, C.O. High-throughput recombinant protein expression in *Escherichia coli*: Current status and future perspectives. *Open Biol.* **2016**, *6*, 160196. [[CrossRef](#)] [[PubMed](#)]
2. Sørensen, H.P.; Mortensen, K.K. Advanced genetic strategies for recombinant protein expression in *Escherichia coli*. *J. Biotechnol.* **2005**, *115*, 113–128. [[CrossRef](#)] [[PubMed](#)]
3. Rosano, G.L.; Ceccarelli, E.A. Recombinant protein expression in *Escherichia coli*: Advances and challenges. *Front. Microbiol.* **2014**, *5*, 172. [[CrossRef](#)] [[PubMed](#)]
4. Sezonov, G.; Joseleau-Petit, D.; D'Ari, R. *Escherichia coli* physiology in Luria-Bertani broth. *J. Bacteriol.* **2007**, *189*, 8746–8749. [[CrossRef](#)] [[PubMed](#)]
5. Daegelen, P.; Studier, F.W.; Lenski, R.E.; Cure, S.; Kim, J.F. Tracing Ancestors and Relatives of *Escherichia coli* B, and the Derivation of B Strains REL606 and BL21(DE3). *J. Mol. Biol.* **2009**, *394*, 634–643. [[CrossRef](#)] [[PubMed](#)]
6. Fulcrand, G.; Dages, S.; Zh, X.; Chapagain, P.; Gerstman, B.S.; Dunlap, D.; Leng, F. DNA supercoiling, a critical signal regulating the basal expression of the lac operon in *Escherichia coli*. *Sci. Rep.* **2016**, *6*, 19243. [[CrossRef](#)]
7. Studier, F.W.; Moffatt, B.A. Use of Bacteriophage-T7 Rna-Polymerase to Direct Selective High-Level Expression of Cloned Genes. *J. Mol. Biol.* **1986**, *189*, 113–130. [[CrossRef](#)]
8. Studier, F.W. Use of bacteriophage T7 lysozyme to improve an inducible T7 expression system. *J. Mol. Biol.* **1991**, *219*, 37–44. [[CrossRef](#)]
9. Dubendorff, J.W.; Studier, F.W. Controlling basal expression in an inducible T7 expression system by blocking the target T7 promoter with *lac* repressor. *J. Mol. Biol.* **1991**, *219*, 45–59. [[CrossRef](#)]

10. Popov, M.; Petrov, S.; Nacheva, G.; Ivanov, I.; Reichl, U. Effects of a recombinant gene expression on ColE1-like plasmid segregation in *Escherichia coli*. *BMC Biotechnol.* **2011**, *11*, 18. [[CrossRef](#)]
11. Teich, A.; Lin, H.Y.; Andersson, L.; Meyer, S.; Neubauer, P. Amplification of ColE1 related plasmids in recombinant cultures of *Escherichia coli* after IPTG induction. *J. Biotechnol.* **1998**, *64*, 197–210. [[CrossRef](#)]
12. Juhas, M.; Ajioka, J.W. Lambda Red recombinase-mediated integration of the high molecular weight DNA into the *Escherichia coli* chromosome. *Microb. Cell Fact.* **2016**, *15*, 172. [[CrossRef](#)] [[PubMed](#)]
13. Juhas, M.; Ajioka, J.W. Flagellar region 3b supports strong expression of integrated DNA and the highest chromosomal integration efficiency of the *Escherichia coli* flagellar regions. *Microb. Biotechnol.* **2015**, *8*, 726–738. [[CrossRef](#)] [[PubMed](#)]
14. Striedner, G.; Pfaffenzeller, I.; Markus, L.; Nemecek, S.; Grabherr, R.; Bayer, K. Plasmid-free T7-based *Escherichia coli* expression systems. *Biotechnol. Bioeng.* **2010**, *105*, 786–794.
15. Fink, M.; Vazulka, S.; Egger, E.; Jarmer, J.; Grabherr, R.; Cserjan-Puschmann, M.; Striedner, G. Micro-bioreactor cultivations of Fab producing *Escherichia coli* reveal genome-integrated systems as suitable for prospective studies on direct Fab expression effects. *Biotechnol. J.* **2019**, *14*, e1800637. [[CrossRef](#)]
16. St-Pierre, F.; Cui, L.; Priest, D.G.; Endy, D.; Dodd, I.B.; Shearwin, K.E. One-Step Cloning and Chromosomal Integration of DNA. *ACS Synth. Biol.* **2013**, *2*, 537–541. [[CrossRef](#)]
17. Dvorak, P.; Chrast, L.; Nikel, P.I.; Fedr, R.; Soucek, K.; Sedlackova, M.; Chaloupkova, R.; de Lorenzo, V.; Prokop, Z.; Damborsky, J. Exacerbation of substrate toxicity by IPTG in *Escherichia coli* BL21(DE3) carrying a synthetic metabolic pathway. *Microb. Cell Fact.* **2015**, *14*, 201. [[CrossRef](#)]
18. Nausch, H.; Huckauf, J.; Koslowski, R.; Meyer, U.; Broer, I.; Mikschofsky, H. Recombinant production of human interleukin 6 in *Escherichia coli*. *PLoS ONE* **2013**, *8*, e54933. [[CrossRef](#)]
19. Gombert, A.K.; Kilikian, B.V. Recombinant gene expression in *Escherichia coli* cultivation using lactose as inducer. *J. Biotechnol.* **1998**, *60*, 47–54. [[CrossRef](#)]
20. Wurm, D.J.; Quehenberger, J.; Mildner, J.; Eggenreich, B.; Slouka, C.; Schwaighofer, A.; Wieland, K.; Lendl, B.; Rajamanickam, V.; Herwig, C.; et al. Teaching an old pET new tricks: Tuning of inclusion body formation and properties by a mixed feed system in *E. coli*. *Appl. Microbiol. Biotechnol.* **2018**, *102*, 667–676. [[CrossRef](#)]
21. Fruchtl, M.; Sakon, J.; Beitle, R. Expression of a collagen-binding domain fusion protein: Effect of amino acid supplementation, inducer type, and culture conditions. *Biotechnol. Prog.* **2015**, *31*, 503–509. [[CrossRef](#)] [[PubMed](#)]
22. Bashir, H.; Ahmed, N.; Khan, M.A.; Zafar, A.U.; Tahir, S.; Khan, M.I.; Khan, F.; Husnain, T. Simple procedure applying lactose induction and one-step purification for high-yield production of rhC1FN. *Biotechnol. Appl. Biochem.* **2016**, *63*, 708–714. [[CrossRef](#)] [[PubMed](#)]
23. Wurm, D.J.; Hausjell, J.; Ulonska, S.; Herwig, C.; Spadiut, O. Mechanistic platform knowledge of concomitant sugar uptake in *Escherichia coli* BL21(DE3) strains. *Sci. Rep.* **2017**, *7*, 45072. [[CrossRef](#)] [[PubMed](#)]
24. Wurm, D.J.; Veiter, L.; Ulonska, S.; Eggenreich, B.; Herwig, C.; Spadiut, O. The *E. coli* pET expression system revisited—mechanistic correlation between glucose and lactose uptake. *Appl. Microbiol. Biotechnol.* **2016**, *100*, 8721–8729. [[CrossRef](#)] [[PubMed](#)]
25. Wurm, D.J.; Marschall, L.; Sagmeister, P.; Herwig, C.; Spadiut, O. Simple monitoring of cell leakiness and viability in *Escherichia coli* bioprocesses—A case study. *Eng. Life Sci.* **2017**, *17*, 598–604. [[CrossRef](#)]
26. Sharan, S.K.; Thomason, L.C.; Kuznetsov, S.G.; Court, D.L. Recombineering: A homologous recombination-based method of genetic engineering. *Nat. Protoc.* **2009**, *4*, 206–223. [[CrossRef](#)]
27. DeLisa, M.P.; Li, J.; Rao, G.; Weigand, W.A.; Bentley, W.E. Monitoring GFP-operon fusion protein expression during high cell density cultivation of *Escherichia coli* using an on-line optical sensor. *Biotechnol. Bioeng.* **1999**, *65*, 54–64. [[CrossRef](#)]
28. Janzen, N.H.; Striedner, G.; Jarmer, J.; Voigtmann, M.; Abad, S.; Reinisch, D. Implementation of a Fully Automated Microbial Cultivation Platform for Strain and Process Screening. *Biotechnol. J.* **2019**, *14*, e1800625. [[CrossRef](#)]
29. Kremling, A.; Bettenbrock, K.; Laube, B.; Jahreis, K.; Lengeler, J.W.; Gilles, E.D. The organization of metabolic reaction networks. III. Application for diauxic growth on glucose and lactose. *Metab. Eng.* **2001**, *3*, 362–379. [[CrossRef](#)]
30. Kremling, A.; Geiselman, J.; Ropers, D.; de Jong, H. Understanding carbon catabolite repression in *Escherichia coli* using quantitative models. *Trends Microbiol.* **2015**, *23*, 99–109. [[CrossRef](#)]

31. Loomis, W.F.J.; Magasanik, B. Glucose-lactose diauxie in *Escherichia coli*. *J. Bacteriol.* **1967**, *93*, 1397–1401. [[CrossRef](#)]
32. Dykhuizen, D.; Hartl, D. Transport by the lactose permease of *Escherichia coli* as the basis of lactose killing. *J. Bacteriol.* **1978**, *135*, 876–882. [[CrossRef](#)]
33. Wilson, D.M.; Putzrath, R.M.; Wilson, T.H. Inhibition of growth of *Escherichia coli* by lactose and other galactosides. *Biochim. Biophys. Acta* **1981**, *649*, 377–384. [[CrossRef](#)]
34. Kopp, J.; Slouka, C.; Ulonska, S.; Kager, J.; Fricke, J.; Spadiut, O.; Herwig, C. Impact of Glycerol as Carbon Source onto Specific Sugar and Inducer Uptake Rates and Inclusion Body Productivity in *E. coli* BL21(DE3). *Bioengineering* **2017**, *5*, 1. [[CrossRef](#)] [[PubMed](#)]
35. Jeong, H.; Barbe, V.; Lee, C.H.; Vallenet, D.; Yu, D.S.; Choi, S.H.; Couloux, A.; Lee, S.W.; Yoon, S.H.; Cattolico, L.; et al. Genome sequences of *Escherichia coli* B strains REL606 and BL21(DE3). *J. Mol. Biol.* **2009**, *394*, 644–652. [[CrossRef](#)] [[PubMed](#)]
36. Sina, M.; Farajzadeh, D.; Dastmalchi, S. Effects of Environmental Factors on Soluble Expression of a Humanized Anti-TNF- α scFv Antibody in *Escherichia coli*. *Adv. Pharm. Bull.* **2015**, *5*, 455–461. [[CrossRef](#)] [[PubMed](#)]
37. Pei, X.-L.; Wang, Q.-Y.; Li, C.-L.; Qiu, X.-F.; Xie, K.-L.; Huang, L.-F.; Wang, A.-M.; Zeng, Z.-W.; Xie, T. Efficient Production of a Thermophilic 2-Deoxyribose-5-Phosphate Aldolase in Glucose-Limited Fed-Batch Cultivations of *Escherichia coli* by Continuous Lactose Induction Strategy. *Appl. Biochem. Biotechnol.* **2011**, *165*, 416–425. [[CrossRef](#)]
38. Tian, H.; Tang, L.; Wang, Y.; Wang, X.; Guan, L.; Zhang, J.; Wu, X.; Li, X. Lactose Induction Increases Production of Recombinant Keratinocyte Growth Factor-2 in *Escherichia coli*. *Int. J. Pept. Res. Ther.* **2011**, *17*, 123–129. [[CrossRef](#)]
39. Huang, L.; Wang, Q.; Jiang, S.; Zhou, Y.; Zhang, G.; Ma, Y. Improved extracellular expression and high-cell-density fed-batch fermentation of chitosanase from *Aspergillus Fumigatus* in *Escherichia coli*. *Bioprocess Biosyst. Eng.* **2016**, *39*, 1679–1687. [[CrossRef](#)]
40. Kim, S.; Cheung, L.H.; Zhang, W.; Rosenblum, M.G. Improved expression of a soluble single chain antibody fusion protein containing tumor necrosis factor in *Escherichia coli*. *Appl. Microbiol. Biotechnol.* **2007**, *77*, 99–106. [[CrossRef](#)]



© 2020 by the authors. Licensee MDPI, Basel, Switzerland. This article is an open access article distributed under the terms and conditions of the Creative Commons Attribution (CC BY) license (<http://creativecommons.org/licenses/by/4.0/>).